Study of different interaction models of double folding potential for $^{6}He+^{12}C$ elastic scattering up to 500 MeV

Ahmed Hammad Amer[1,2]

[1]National Research Nuclear University "MEPHI", Moscow, 115409, Russia

2Physics Department, Faculty of Science, Tanta University, 31527 Tanta, Egypt

E-mail: ahmed.amer@science.tanta.edu.eg

Abstract

Our investigation aims to study different interaction models of double folding potential for 6He+12C nuclear system. The available experimental data for 6He elastically scattered from 12C at energies 5.9, 9.9, 18, 30, 229.8, 249.6 and 493.8 MeV are reanalyzed within the framework of optical model (OM) potential of Woods–Saxon (WS) shape. We created the real part of the nuclear potential using the double folding model (DFM) approach based upon different interaction models such as: CDM3Y6 Paris, DDM3Y1 Reid, BDM3Y1 (Paris and Reid). Among these models, the potential generated by BDM3Y1 Reid is shallower in comparison with the rest, which reflects the necessity to use higher renormalization factor. Energy dependences of both reaction cross section and imaginary potential volume integral are studied. The calculated angular distributions are in a good agreement with the experimental data in the whole angular range.

Introduction

Elastic scattering of the light unstable exotic nuclei on stable target nuclei provides unique information's about the interaction potential between the colliding nuclei and the distributions of nuclear matter density. The nucleus-nucleus potential is an important quantity not only for describing elastic scattering cross sections but also as an ingredient in describing all the phenomena that occur when two nuclei colliding together [1]. The study of a nucleus-nucleus optical potential is one of the main subjects of nuclear physics. particularly, the understanding of the complex optical potential for composite projectiles from a microscopic perspective is extremely necessary, not just to grasp the related reaction dynamics involved, but to develop a practical tool that predicts the optical potential of colliding systems that sometimes do not have elastic scattering measurements, such as in the case of the neutron-rich or proton-rich β-unstable nuclei [2]. Analyses of experimental data on total reaction cross-sections have shown that weakly-bound neutron-rich light nuclei, have larger radii and deviate considerably from the $R \sim A^{1/3}$ rule. It has been realized that such a new phenomenon is due to the weak binding energy of the last few neutrons which form the so-called neutron halo or thick neutron skin. This recent phenomenon (halo) and unusual exotic nuclei structure have become one of the most significant subjects of modern nuclear physics. **Our present study aims to analyze the elastic scattering of halo nucleus ^{6}He from ^{12}C** nucleus at different energies ranging from 5.9 to 493.8 MeV phenomenologically with the optical model (OM) and semi-microscopically using double folding optical potential (DF) of various interaction models such as: CDM3Y6 Paris, DDM3Y1 Reid, BDM3Y1 (Reid and Paris) and comparing between them. The key difference between these interaction models is the parameters values of density-dependent function $F(\rho)$ used in calculating it. We also extracted the renormalization factor N_r of the folding potentials generated using different interaction models at different concerned energies.

Theoretical Calculations

The angular distributions for 6He+12C elastic scattering in energy range 5.9-493.8 MeV are reanalyzed using both phenomenological and semi-microscopic potentials: optical model (OM) potential and double folding (DF) potential of CDM3Y6 Paris, DDM3Y1 Reid, BDM3Y1 (Reid and Paris) interaction models. Firstly, The analyses employed real and imaginary volume central potentials together with a Coulomb potential. The used potential has the following form:

$$U(r) = V_C(r) + V_N(r) = V_C(r) - \frac{V_o}{1+exp\left(\frac{r-R_v}{a_v}\right)} - i\,\frac{W_V}{1+exp\left(\frac{r-R_W}{a_W}\right)}$$

where $V_C(r)$ is the Coulomb potential due to a uniform sphere with charge equal to that of the target nucleus and radius $R_i = r_i A_t^{1/3}$.

Secondly, the available 6He+12C elastic scattering angular distributions are reanalyzed in the framework of double folding optical model (DFOM). the real part of the interaction potential was derived on the basis of DF using code fresco [8]. The potential is calculated from the formula:

$$v^{DF}(r) = \int \rho_p(r_p)\, \rho_t(r_t)\, v_{NN}(r_{pt}) d^3r_p\, d^3r_t\ ,\ r_{pt} = |\boldsymbol{r} + \boldsymbol{r_t} - \boldsymbol{r_p}|$$

where v_{NN} is the effective nucleon- nucleon interaction potential which was taken to be of the CDM3Y6 and BDM3Y1form based on the M3Y-Paris potential:

$$v_D(s) = 11061.625\,\frac{\exp(-4s)}{4s} - 2537.5\,\frac{\exp(-2.5s)}{2.5s},$$

$$v_{EX}(s) = -1524.25\,\frac{\exp(-4s)}{4s} - 518.75\,\frac{\exp(-2.5s)}{2.5s} - 7.8474\,\frac{\exp(-0.7072s)}{0.7072\,s},$$

and also was taken to be of the DDM3Y1 and BDM3Y1 form based on the M3Y- Reid potential:

$$v_D(s) = 7999.0\frac{\exp(-4s)}{4s} - 2134.25\,\frac{\exp(-2.5s)}{2.5s},$$

$$v_{EX}(s) = -4631.38\,\frac{\exp(-4s)}{4s} - 1787.13\,\frac{\exp(-2.5s)}{2.5s} - 7.8474\,\frac{\exp(-0.7072s)}{0.7072\,s},$$

The M3Y-Paris and M3Y- Reid interactions are scaled by an explicit density-dependent function F(ρ):

$$v_{D(EX)}(s,\rho) = F(\rho) v_{D(EX)}(s)$$

where (v_D, v_{EX}) are represents the direct and exchange terms of the M3Y-Paris, ρ is the density distribution of nuclear matter (NM). Density-dependent function $F(\rho)$, was considered to have an exponential dependence, and the parameters of this function, were adjusted to reproduce the NM saturation properties in the calculations of Hartree–Fock. The density-dependent function can be written as:

$$F(\rho) = C[1 + \alpha\exp(-\beta\rho) - \gamma\rho^n],$$

The parameters C, α, β, γ of these interaction models are tabulated in table 1 taken from [7].

Table I – Parameters of density-dependence function $F(\rho)$

Interaction model	C	α	$\beta(fm^3)$	$\gamma(fm^{3n})$	n	$K(MeV)$
CDM3Y6 Paris	0.2658	3.8033	1.4099	4.0	1	252
DDM3Y1 Reid	0.2845	3.6391	2.9605	0.0	0	171
BDM3Y1 Reid	1.2253	0.0	0.0	1.5124	1	232
BDM3Y1Paris	1.2521	0.0	0.0	1.7452	1	270

The density distribution of 6He nucleus is calculated using four Gaussian terms from the following expression

$$\rho_{6He}(r) = \sum_{K=1}^{4} C_K.\exp(-(r/a_k)^2),$$

This formula gives a root mean square (rms) radius $\langle r^2\rangle^{\frac{1}{2}} = \mathbf{2.48}\,fm$.

Table : Parameters of ^{6}He density in Eq. (11) taken from Ref. **[18]**

C_K	**5.6344048E-5**	**0.242375**	**1.3300797E-3**	**2.545367E-2**
a_k	5.773427	1.414237	3.79652	2.314934

The density distribution of 12C is expressed in the two-parameter Fermi function form as:

$$\rho(r) = \frac{\rho_o}{1+\exp\left(\frac{r-c}{z}\right)},$$

With ($\rho_o = 0.207\,fm^{-3}$,c=2.1545fm and z=0.425 fm) ; these parameters were adjusted in order to have a root mean square (rms) radius $\langle r^2\rangle^{\frac{1}{2}} = 2.298\,fm$. Finally, the generated folding potentials were fed into the computer code FRESCO [8] to calculate elastic scattering differential cross sections. The selection of optimal potential parameters was carried out based on minimizing the deviation between the theoretical calculations and the experimental angular distributions data using chi-square χ^2, criteria, which defined by

$$\chi^2 = \frac{1}{N}\sum_{i=1}^{N}\left[\frac{\sigma_{th}(\theta_i) - \sigma_{exp}(\theta_i)}{\Delta\sigma_{exp}(\theta_i)}\right]^2,$$

Where N is the number of differential cross section data points and $\sigma_{th}(\theta_i)$ is the calculated cross section at angles (θ_i) . $\sigma_{exp}(\theta_i)$ and $\Delta\sigma_{exp}(\theta_i)$ are the corresponding experimental cross section and its relative uncertainty, respectively. The χ^2 values were obtained considering uniform 10% errors for all the analyzed data. The volume integrals are currently used as a sensitive measure of the potential strength. In the present work, we apply this quantity to the real and imaginary parts of optical potential and expressed as $J_V$and J_W respectively:

$$J_V(E) = \frac{4\pi}{A_P A_T}\int_0^\infty V(r)\, r^2\, dr,\ J_W(E) = \frac{4\pi}{A_P A_T}\int_0^\infty W(r)\, r^2\, dr$$

Where A_P and A_T are mass numbers of the projectile and target, respectively.

Results and Discussion

The comparisons between the experimental angular distribution data for 12C(6He,6He) 12C elastic scattering at energies (5.9 MeV [11], 9.9 MeV[12], 18 MeV [13], 30 MeV [14], 229.8 MeV [5], 249.6MeV[8] and 493.8 MeV [15]) and the theoretical predictions within the framework of phenomenological OM-WS and (DFM) of different interaction potential models such as: DDM3Y1 Reid, CDM3Y6 Paris, BDM3Y1 Reid, and BDM3Y1 Paris are shown in Fig.2.Both phenomenological (OM) and semi-microscopic (DFM) calculations were performed using computational code SFRESCO [20].The OM analysis of the experimental data was performed by using Woods-Saxon (WS) forms for both real and imaginary parts of the potential where the radii r_v=1.276 fm and r_w=1.846 fm were fixed taken from [22], and only the four remaining parameters (Vo, Wv, av, aw) were varied.

In (DFM) calculations, the optimal potential parameters for the imaginary part extracted from the OM were kept fixed. In other words, the fitting process was performed using only one free parameter Nr "renormalization factor for the real part". The radius parameter for the Coulomb potential (r_C) was fixed at 1.276 fm. The optimal six optical potential parameters and the values of volume integrals for the real part (JV) and imaginary part (JW) of the of the optical potential as well as the values of reaction cross sections σR that are calculated from both OM and DFM (of different interaction Models) are listed in Table 3. Also, in table 3 we can see the best fit renormalization factor (Nr) for 12C(6He,6He) 12C elastic scattering system which ranges between 0.556 and 0.9018. A general look of Fig.2. show that at all studied energies, our OM-WS and DFM of different interaction models potentials reasonably reproduced the elastic angular distributions in the whole angular range, except in the forward small angles between (〖1.12〗^°- 〖4.12〗^°)at E= 493.8 MeV. Furthermore, all the normalized folding potential of different interaction models predicted correctly the magnitude of the cross section as well as the places of minima and maxima at energies E = 18, 30, 229.8 and 249.6 MeV and successfully described the refractive behavior (i.e. the experimental elastic differential cross sections divided by Rutherford cross sections dσ⁄〖dσ〗_R increases with increasing scattering angle) , which observed at E=229.8 MeV.

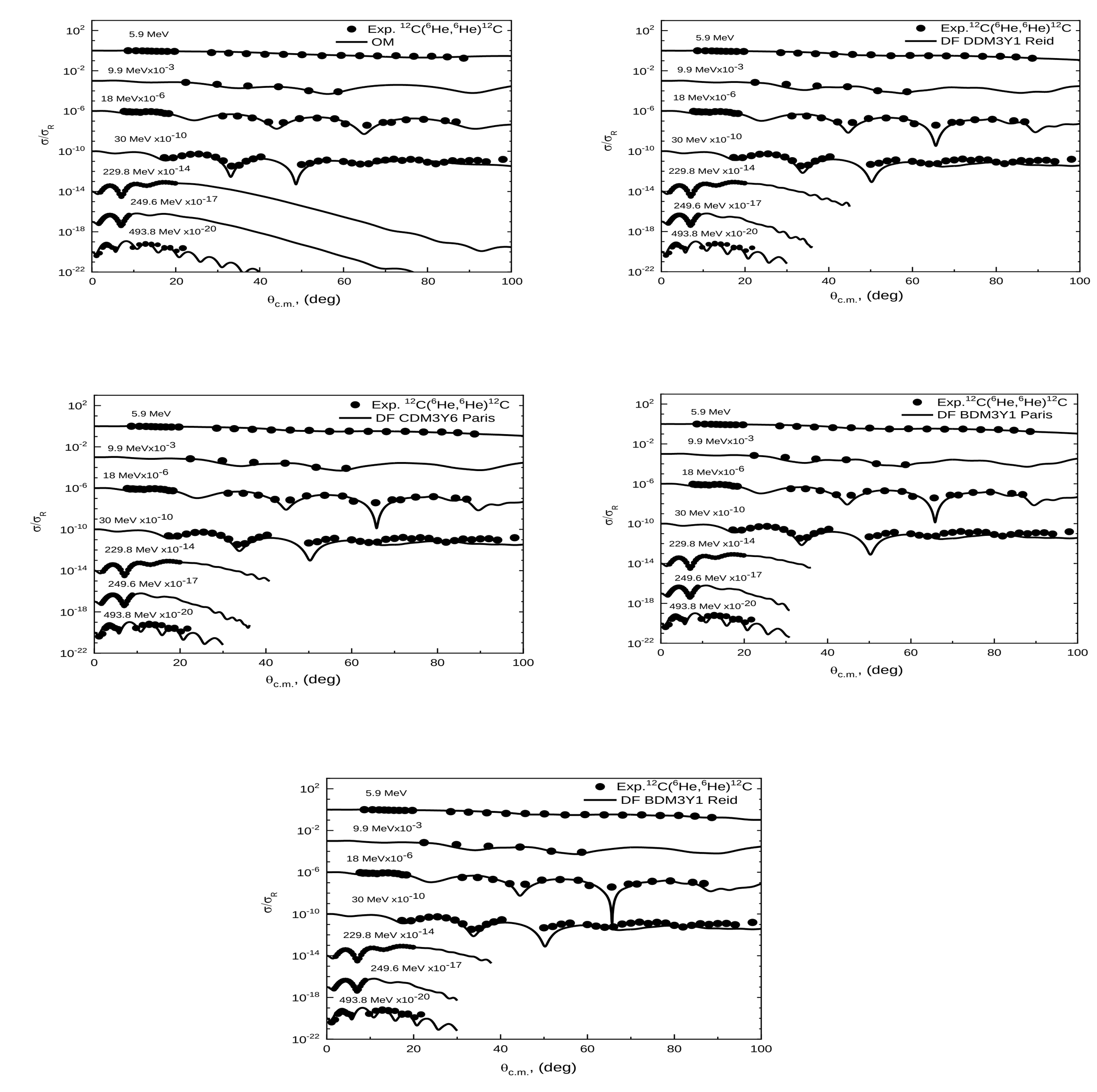

Fig. 2. Show the comparisons between the experimental data (solid circles) for $^{6}He + ^{12}C$ elastic scattering at energies (5.9, 9.9, 18, 30, 229.8, 249.6 and 493.8 MeV) and the theoretical calculations(colored dotted lines) within the framework of OM and DFM of different interaction models.

Summary

We reanalyzed the experimental angular distributions for $^{6}He+^{12}C$ nuclear system at energies 5.9, 9.9, 18, 30, 229.8, 249.6 and 493.8 MeV using the (OM) potential in which the real and imaginary parts have a Woods-Saxon shape and also using the (DFM) potential of different interaction models CDM3Y6 Paris , DDM3Y1 Reid, , BDM3Y1 (Paris and Reid). However, Among these interaction models, the Potential generated by BDM3Y1 Reid interaction model is shallower in comparison with the rest, which reflects the necessity to use higher renormalization factor, on the other hand, the potential created by CDM3Y6 Paris model of interaction is the deepest one which reflects the necessity to use lower renormalization factor except that the first two low energies at (5.9 and 9.9) MeV , where the DDM3Y1 Reid was the deepest one. We noticed that, the calculated imaginary potential volume integrals of $^{6}He+^{12}C$ elastic scattering, increases with increasing energy of ^{6}He. The total reaction cross section σ_R behaves two different behaviors over the studied energy range, where it increases with increasing energy up to 30 MeV ^{6}He projectile and starts to decrease from E=30 MeV to the last high energy 493.8 MeV. We concluded that, all the extracted normalized folding potential of different interaction models predicted correctly the magnitude of the cross section as well as the places of minima and maxima at energies E = 18, 30, 229.8 and 249.6 MeV and successfully described the refractive behavior, which observed at E=229.8 MeV. Good agreement between the experimental data and the theoretical calculations in the whole angular range at all energies, except in the forward small angles between $(1.12^{\circ} - 4.12^{\circ})$at E= 493.8 MeV.

References

1. G. R. Satchler and W. G. Love, "Folding model potentials from realistic interactions for heavy-ion scattering," Phys. Rep. 55, 183 (1979).
2. Dong Hong-Fei, MA Yin-Qun, and MA Zhong-Yu, Elastic scattering of ^{6}He from ^{12}C at 38.3 MeV/nucleon, Chinese Physics C, 33, 532 (2009).
3. Zakaria M. M. Mahmoud, Awad A. Ibraheem And Sherif R. Mokhtar, Folding Model Analysis Of ^{6}he + ^{120}sn Elastic Scattering, International Journal of Modern Physics E, 22, 1350086 (2013).
4. Y. Ogawa, K. Yabana, and Y. Suzuki, Glauber model analysis of the fragmentation reaction cross sections of ^{11}Li, Nucl. Phys. A 543, 722 (1992).
5. V. Lapoux et al, Coupling effects in the elastic scattering of ^{6}He on ^{12}C, Phys.Rev.C 66, 034608 (2002).
6. M.Aygun, Y.Kucuk, I.Boztosun, and Awad A.Ibraheem, Microscopic few-body and Gaussian-shaped density distributions for the analysis of the ^{6}He exotic nucleus with different target nuclei, Nucl. Phys. A 848, 245–259 (2010).
7. A.M. Sánchez Benítez et al, Scattering of ^{6}He at energies around the Coulomb barrier, J. Phys. G: Nucl. Part. Phys. 31, S1953 (2005).
8. J.S. Al-Khalili et al, Elastic scattering of ^{6}He and its analysis within a four-body eikonal model, Physics Letters, B 378, 45-49 (1996).
9. R.J. Smith et al, Scattering of ^{6}He from ^{197}Au, ^{nat}Ti, ^{27}Al, ^{nat}C, and ^{9}Be at E = 8-9 MeV ,Phys. Rev. C 43, 761-765 (1991).
10. Zakaria M. M. Mahmoud, Awad A. Ibraheemb, and M. ElAzab Farid, Optical Model Analysis of p+^{6}He Scattering over a Wide Range of Energy, Physics of Particles and Nuclei Letters 11, 219 (2014).
11. A.N.Ostrowski et al, Low-energy radioactive ion beam induced nuclear reactions, J. Phys. G: Nucl. Part. Phys. 24, 1553–1559 (1998).
12. R. E. Warner et al, Elastic scattering of 10 MeV ^{6}He from ^{12}C, ^{nat}Ni, and ^{197}Au, Phys. Rev. C 51,178-181 (1995)
13. M.Milin et al, the ^{6}He scattering and reactions on ^{12}C and cluster states of ^{14}C, Nucl. Phys. A 730, 285–298 (2004).
14. D. Smalley et al, Two-neutron transfer reaction mechanisms in $^{12}C(^{6}He,^{4}He)^{14}C$ using a realistic three-body ^{6}He model, Phys. Rev. C 89, 024602(2014).
15. J. L. Lou, Y. L. Ye, D. Y. Pang et al, Proceedings of the ^{14}th National Conference on Nuclear Structure in China , P.158 (2012) ; J. L. Lou, Y. L. Ye, D. Y. Pang et al, Quasi elastic scattering of ^{6}He from ^{12}C at 82.3 MeV/nucleon, Phys. Rev. C, 83: 034612 (2011).
16. Awad A. Ibraheem, Folding model calculations for $^{6}He+^{12}C$ elastic scattering, Chinese Physics C 40, 034102 (2016).
17. Dao T Khoa, W von Oertzen, H G Bohlen, and S Ohkubo, Nuclear rainbow scattering and nucleus -nucleus potential, J. Phys. G: Nucl. Part. Phys. **34,** R143 (2007).
18. B. Abu-Ibrahim, K. Fujimura, Y. Suzuki, Calculation of the complete Glauber amplitude for p+^{6}He scattering, Nucl. Phys. A 657, 391-410 (1999).
19. M. El-Azab Farid and G.R. Satchler, a density-dependent interaction in the folding model for heavy-ion potentials, Nucl. Phys. A 438, 525 (1985).
20. I. J. Thompson, "Coupled reaction channels calculations in nuclear physics," Comput. Phys. Rep. 7, 167 (1988).
21. A.J. Koning, and J.P. Delaroche, Local and global nucleon optical models from 1 keV to 200 MeV, Nucl. Phys. A 713, 231–310(2003).